JOURNAL OF APPLIED ELECTROCHEMISTRY **27** (1997) 1012–1020

An indirect electrochemical process for the removal of NO_x from industrial waste gases

K. -H. KLEIFGES, G. KREYSA, K. JÜTTNER,

Karl-Winnacker-Institut der DECHEMA e.V., PO Box 15 01 04, D-60061 Frankfurt am Main, Germany

Received 20 August 1996; revised 17 October 1996

The development of a new electrochemical process for the absorption of NO_x from industrial waste gases is described. Conversion of NO was performed by an indirect outer cell process using dithionite as the redox mediator and $Fe^{III}EDTA$ as the complexing agent. The absorption process, involving complex formation with $Fe^{III}EDTA$ in the absence and presence of dithionite, was investigated using a packed bubble column. In semibatch experiments the dependence of different system parameters on the degree of NO conversion was studied: concentration of dithionite and $Fe^{III}EDTA$, gas flow rate, oxygen content, and temperature. The reaction products in the gas phase and in the liquid phase were analyzed using gas chromatography and ion chromatography, respectively. This analysis proved that, instead of N_2 or N_2O, ammonia and amidosulfonic acid are the main reaction products in the solution. The kinetics and the conditions for the regeneration of dithionite by electrochemical reduction of sulfite were studied on RDE and by experiments in a divided cell. For the dithionite production a current efficiency of about 80% was found in 0.2 M Na_2SO_4 at pH 5.6. By combining the chemical NO absorption in a gas/liquid contactor with the electrochemical regeneration of dithionite in a divided plate and frame cell a degree of NO conversion better than 90% under continuous operation can be obtained.

List of symbols

c	concentration (mol dm^{-3})
c_A^0	initial concentration of species A (mol dm^{-3})
D	diffusion coefficient (cm^2 s^{-1})
D^{calc}	calculated diffusion coefficient (cm^2 s^{-1})
E	potential (V)
E_s	specific energy consumption (kWh m^{-3})
E_0^0	standard potential (V)
F	Faraday's constant (96 487 C mol^{-1})
H	Henry coefficient (mol dm^{-3} Pa^{-1})
I	current intensity (A)
i	current density (mA cm^{-2})
K	complex-formation constant (dm^3 mol^{-1})
k^0	mass transfer coefficient (cm s^{-1})
p	partial pressure (Pa)
q^g	gas flow rate (dm^3 min^{-1})
q^l	liquid flow rate (dm^3 min^{-1})
R	universal gas constant (J mol^{-1} K^{-1})
T	temperature (K)
t	time (s)
U_c	cell voltage (V)
V	volume (dm^3)
V^l	volume of the liquid phase (dm^3)
V_R	reactor volume (dm^3)
v	normalized space velocity (dm^3 h^{-1} dm^{-3})
X	degree of conversion

Greek symbols

α_c	symmetry factor of the cathode reaction
δ^l	diffusion layer thickness(cm)
ε	gas hold-up
Φ^e	current efficiency
ν	kinematic viscosity (cm^2 s^{-1})
ν_e	overall reaction valency
ω	rotation frequency (s^{-1})

Subscript

*	gas/liquid interphase

1. Introduction

More stringent regulations governing the emission of toxic gases from industrial sources have evoked an increasing demand for new and efficient abatement techniques. The well-established conventional wet and dry processes which are applied for the removal of SO_2 and NO_x in large-scale power plants are not flexible enough to cope with the varying conditions of discontinuously operating smaller scale heating combustion units, chemical plants or extremely dusty waste gases. Examples are the emissions from glass manufacturing, cement or limestone production, heat treatment and surface processing of metals, nitric acid production or mineral oil refineries. This situation has encouraged the development of new electrochemical concepts for gas purification as an alternative to conventional chemical techniques where the toxic components of off-gases are converted by catalytic or noncatalytic oxidation or by

0021-891X

reduction reactions to nontoxic components or products [1–7]. An inherent advantage of electrochemical processes is the conversion of chemical components either directly or indirectly by an electrochemical inner-cell or outer-cell process [8–18] where the electron as a 'clean reagent' is the counterpart of redox chemicals, of which huge amounts are added in most of the conventional chemical processes. Other advantages which make electrochemical processes attractive are their versatility, energy efficiency, amenability to automation and cost effectiveness.

The basic principles of electrochemical gas purification and several examples of processes which have been developed and tested either in the laboratory or applied on an industrial scale can be found in the literature and are not repeated here [9,10,12].

The results presented in this paper deal with the development of a new electrochemical process for the removal of NO_x as part of an overall process for the simultaneous removal of SO_2 and NO_x [17–20]. The experiments described were restricted to the treatment of nitrogen monoxide, NO, which is the main component (95%) of the nitrogen oxides found in combustion gases.

2. Experimental details

The experiments for studying the absorption and conversion of NO were performed in a cylindrical perspex glass laboratory column 11 cm in diameter filled with a packing of Raschig rings (dia. 1.5 cm) 46 cm high. A packing of glass spheres (dia. 1 cm) at the inlet served as the gas distributor to avoid channel flow formation. The temperature was controlled by a cryostat (Haake) and a cooling coil around the column. The composition of the gas phase with respect to N_2, N_2O or O_2 at the inlet and outlet of the column was measured discontinuously by a gas chromatograph (Carlo Erba) in combination with an integrator (Spectra Physics 4270). Continuous analyses of the NO and NO_x content were carried out with an NO_x analyser (Beckmann). In all the experiments helium was used as the carrier gas to allow a sensitive proof of N_2 as a possible reaction product. To simulate realistic conditions, O_2 was present at a magnitude of a few per cent in most experiments.

In the case of test gas mixtures containing NO and O_2 as individual components, the formation of NO_2 by gas phase reactions was largely suppressed by establishing the NO mixture with the carrier gas first and finally adding the oxygen just in front of the inlet. The dosing and gas flow rates were adjusted by mass flow controllers (Hastings, HFC202). The composition of the solution was analysed by means of atomic absorption spectroscopy AAS (Perkin Elmer 1100B) and ion chromatography IC (Dionex 2000i/SP).

Kinetic investigations of the electrochemical dithionite regeneration were made on lead electrodes in a conventional three-electrode cell under potentiostatic control using a rotating disc electrode RDE. The current efficiency Φ^e for the regeneration of dithionite was measured in a divided cell with a cation exchange membrane (Thomapor, 50382), a porous lead cathode of 84 cm^2 geometrical electrode area as the working electrode and an expanded metal sheet anode made of titanium dioxide as the counter electrode. An Ag/AgCl electrode ($E_o = 0.207$ V) served as the reference electrode in combination with a Luggin capillary. All potentials quoted refer to the standard hydrogen electrode (SHE).

On a laboratory scale the regeneration of dithionite was performed in closed loop experiments under galvanostatic conditions using a plate and frame cell (Electro Cell AB, SU Electro MP Cell) with a lead electrode of 0.01 m^2 area and a cation exchanger membrane. The lead electrodes were activated by cathodic pre-electrolysis with $I = -3$ A in 0.2 M Na_2SO_4-solution.

3. Results and discussion

3.1. *Overall process scheme*

From the viewpoint of process engineering there are several alternative methods of carrying out an electrochemical gas purification process. In any case, the pollutant species must be transferred from the gas phase into a liquid phase of an electrolyte where the conversion can take place either by direct electrochemical reduction or oxidation at the cathode or anode of an electrochemical cell or by an indirect reaction mechanism where the pollutant species is converted via a redox mediator system. The redox mediator may be present at a remarkably higher concentration and homogeneously dissolved in the purging solution or as a heterogeneous catalyst. In both cases the redox mediator must be regenerated by an electrochemical reaction. The indirect process offers the advantage of higher space/time yield because the whole bulk of the solution acts as a reaction space, whereas in the direct process the space/time yield is limited by the specific electrode area. Both the direct and indirect electrochemical conversion with regeneration of the redox mediator can be achieved by an inner-cell or outer-cell process.

Figure 1 shows the scheme of the NO_x conversion process which is the subject of the present investigation of NO_x removal. It represents a typical outer-cell process consisting of an absorption column and an electrochemical cell for the regeneration of the redox mediator. The absorption column contains dithionite as the homogeneous redox mediator by which the NO molecule is reduced in the liquid phase. To improve the solubility of the nitrogen monoxide, $Fe^{(II)}EDTA$ is present in the solution as a complexing agent. The scrubber is designed as a packed bubble column to improve the mixing of the gas and the liquid phases by turbulence promoters. The absorption liquid is pumped through the cathode compartment of an electrochemical plate and frame cell, where the sulfite SO_3^{2-}, which is formed by the homogeneous reaction of NO with dithionite, is regenerated at the cathode

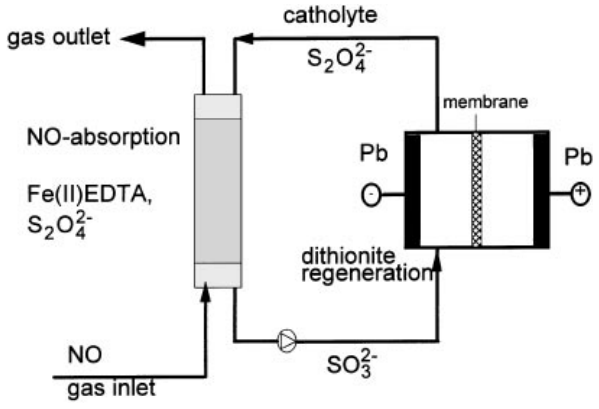

Fig. 1. Scheme of the indirect process for removal of NO_x with dithionite as the redox mediator and $Fe^{(II)}EDTA$ as the complexing agent.

to dithionite. The regenerated absorption solution re-enters the absorption column under counter current flow conditions with respect to the gas flow direction.

The processes which take place at different parts of the gas purification reactor have been studied separately in detail and the results will be described in the following.

3.2. *NO absorption*

An intricate problem of all wet processes is the low solubility of NO in aqueous solutions. This is indicated by the low value of the Henry coefficient H which at room temperature ($T = 298$ K) is found in the range of 1.01×10^{-8} mol dm^{-3} Pa^{-1} $\leq H \leq 1.92 \times 10^{-8}$ mol dm^{-3} Pa^{-1} [21]. This is about three orders of magnitude lower than the Henry coefficient of sulfur dioxide. The physical solubility of NO cannot be substantially improved either by variation of the pH within the range $0 \leq$ pH ≤ 13 or by decreasing the temperature; for example, in the temperature range of $T = 283$–363 K the Henry coefficient (H) varies in the range $(2.55$–$0.37) \times 10^{-8}$ mol dm^{-3} Pa^{-1} [22]. To increase the mass transfer of NO from the gas phase into the liquid phase, the absorption equilibrium at the gas/liquid phase boundary must be disturbed by a chemical reaction by which NO is continuously withdrawn from the interphase leading to a change in the concentration profile within the boundary layer and a modification of the transport equations (see Fig. 2). Depending on whether highly oxidizing reagents like $KMnO_4$, $NaClO_2$, NaClO, H_2O_2, $K_2Cr_2O_7$, Ce (IV) or reducing agents like $Na_2S_2O_4$ are used for the oxidation or reduction of NO, the wet chemical processes can be divided into absorption–reduction or absorption–oxidation processes [23].

Another possibility is the oxidation of NO in the gas phase, leading to a more soluble species such as NO_2 or N_2O_3 [24]. This approach was implemented in the Walter simultaneous process where NO is oxidized with ozone to NO_2 which is then converted to NH_4NO_3 after absorption in a solution containing aerated ammonia [25].

In the present investigation the absorption–reduction pathway was followed using dithionite $S_2O_4^{2-}$ as the reducing agent. Figure 3 shows a semibatch absorption experiment with dithionite in the absorption liquid where the gas phase contains a fixed concentration of NO (0.07 vol%) and O_2 (3 vol%) at the inlet. Comparing the concentration transients of NO and NO_x at the outlet in Fig. 3(a) with the corresponding transients of $S_2O_4^{2-}$, SO_3^{2-} and SO_4^{2-} in the liquid phase, Fig. 3(b), the absorption of NO is limited and disappears almost completely when the dithionite is consumed. During the continuous decrease of $S_2O_4^{2-}$ the degree of NO absorption varies between 30% and 50%. The overall consumption of $S_2O_4^{2-}$, corresponding to 0.306 mol compared with the amount of 0.036 mol of absorbed NO, indicates that the greater part of the dithionite is consumed by other reactions. This is also evident from the simultaneous formation of SO_4^{2-} in Fig. 3(b) and from a similar experiment shown in Fig. 4(a) and (b) which was performed in the absence of NO. In this experiment absorption of O_2 takes place as long as $S_2O_4^{2-}$ is

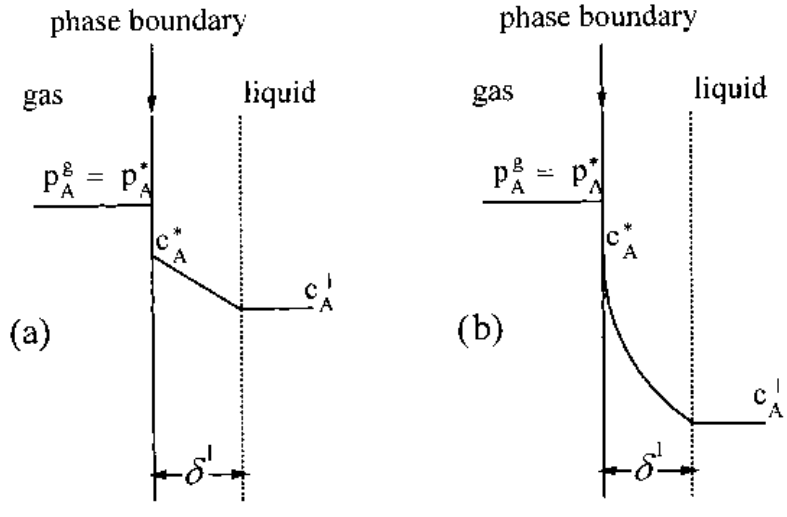

Fig. 2. Concentration profiles at the gas / liquid phase boundary: (a) physical absorption and (b) reaction controlled mass transfer of species A.

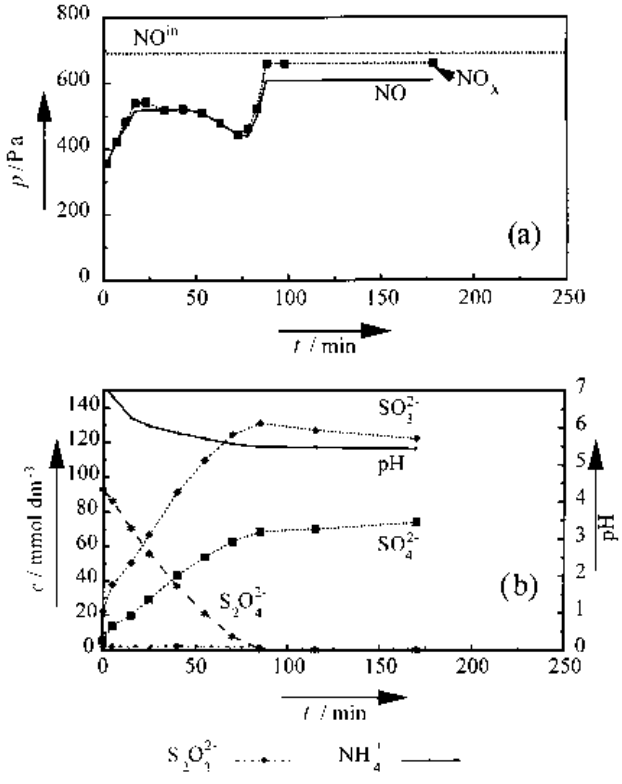

Fig. 3. Semibatch experiment of NO absorption with $S_2O_4^{2-}$ as the reducing agent: (a) gas-phase analysis and (b) solution analysis. System parameters: gas flow rate $q^g = 4.56\,dm^3\,min^{-1}$, partial pressure of oxygen $p_{O_2} = 2.9\,kPa$, volume of the liquid phase $V^l = 3.3\,dm^3$, gas holdup $\varepsilon = 0.046$, $T = 313\,K$, absorption liquid buffered with citric acid/citrate.

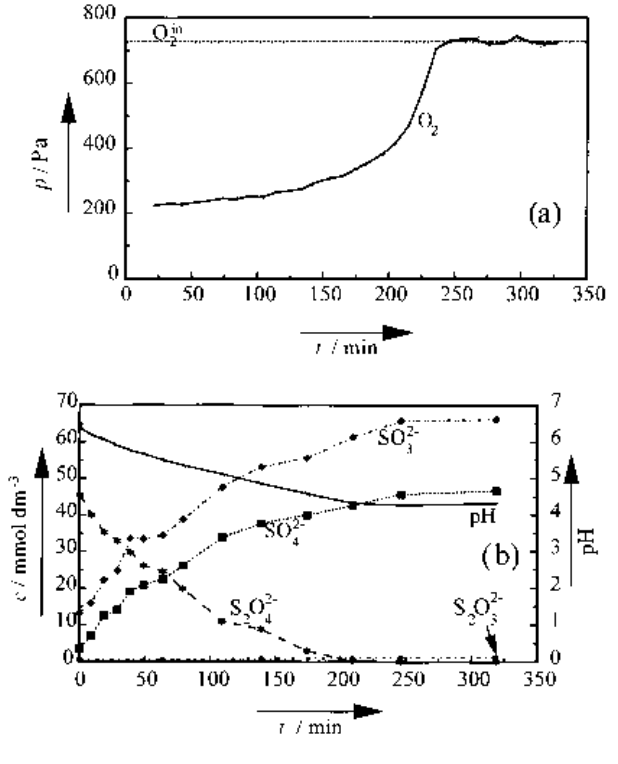

Fig. 4. Semibatch experiment of O_2 absorption with $S_2O_4^{2-}$ as the reducing agent in the absence of NO: (a) gas-phase analysis and (b) solution analysis. System parameters: gas flow rate $q^g = 3.93\,dm^3\,min^{-1}$, volume of the liquid phase $V^l = 3.3\,dm^3$, gas holdup $\varepsilon = 0.048$, $T = 313\,K$, absorption liquid buffered with citric acid/citrate.

present in the solution, leading to the formation of SO_4^{2-} and SO_3^{2-} according to the following reaction:

$$S_2O_4^{2-} + H_2O + O_2 \longrightarrow SO_4^{2-} + SO_3^{2-} + 2\,H^+ \quad (1)$$

The deviation of the concentration ratio $[SO_3^{2-}]/[SO_4^{2-}]$ from unity implies a competitive reaction [26]:

$$2\,S_2O_4^{2-} + 2H_2O + O_2 \longrightarrow 4\,HSO_3^- \quad (2)$$

These results demonstrate the fact that the reduction of NO by dithionite in the presence of oxygen is not selective and yields only low degrees of NO conversion.

To improve the selectivity and efficiency of the absorption process, experiments with different metal chelate complexes ($Fe^{(II)}$EDTA, $Co^{(II)}$EDTA, $Co^{(II)}$-triethylenetetraamine) were carried out to increase the mass transfer of NO and its concentration in the solution. The most promising results were found with $Fe^{(II)}$EDTA. Figure. 5 shows a typical absorption experiment with $Fe^{(II)}$EDTA in the absence of $S_2O_4^{2-}$, indicating the absorption of NO by the formation of a complex according to

$$Fe^{(II)}EDTA + NO \rightleftharpoons Fe^{(II)}EDTA(NO) \quad (3)$$

From the graphic integration of the absorption curve in Fig. 5 the overall amount of absorbed NO, $\Delta c_{NO,abs}$, was determined, and by using the known Henry coefficient $H = 1.47 \times 10^{-8}\,mol\,dm^{-3}\,Pa^{-1}$, the complex-formation constant K of Reaction 3 could be calculated from the following equations:

$$K = \frac{c_{Fe^{II}EDTA(NO)}}{c_{Fe^{II}EDTA} \times c_{NO}} \quad (4)$$

through mass balance, to

$$K = \frac{\Delta c_{NO,abs} - Hp^g_{NO}}{\left(c^0_{Fe^{II}EDTA} - \Delta c_{NO,abs} + Hp^g_{NO}\right) \times Hp^g_{NO}} \quad (5)$$

A value of $K = 1.36 \times 10^6\,dm^3\,mol^{-1}$ was found, which means that under these conditions the solubility of NO is enhanced by a factor of 2.6×10^3 with respect to the physical solubility of NO. After attaining the equilibrium state of the complexation process (Equation 3) no further absorption of NO

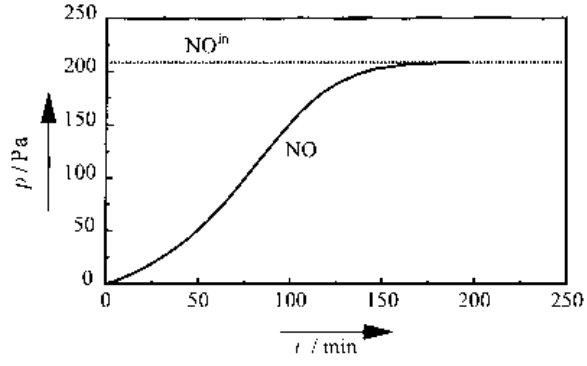

Fig. 5. Semibatch experiment of NO absorption by complex formation with $Fe^{(II)}$EDTA. System parameters: gas flow rate $q^g = 3.63\,dm^3\,min^{-1}$, volume of the liquid phase $V^l = 3.2\,dm^3$, gas holdup $\varepsilon = 0.044$, $T = 313\,K$, pH 7.0, $c_{Fe^{(II)}EDTA} = 9.1\,mmol\,dm^{-3}$.

takes place. It is therefore necessary to combine this reaction with a redox process to withdraw the dissolved NO continuously from the $Fe^{(II)}EDTA(NO)$ complex, thus disturbing the adjustment of the absorption equilibrium. To obtain a suitable redox mediator, dithionite was combined with $Fe^{(II)}EDTA$, leading to an enhanced conversion of NO as demonstrated by the batch experiment in Fig. 6. In comparison with the experiment in the absence of $Fe^{(II)}EDTA$, Fig. 3(a), there is a marked increase in the degree of NO conversion, $X = 0.9$, which remains almost constant as long as dithionite is present in the solution (cf. Fig. 6(a) and (b)). The excess of the SO_3^{2-} over SO_4^{2-} in Fig. 6(b) is higher than that found in the experiment without $Fe^{(II)}EDTA$ (Fig. 3(b)) which in addition to Equations 4 and 5 can be attributed to the following reaction:

$$2Fe^{(III)}EDTA + S_2O_4^{2-} + 2H_2O \longrightarrow 2Fe^{(II)}EDTA + 2SO_3^{2-} + 4H^+ \quad (6)$$

where $Fe^{(III)}EDTA$ is the oxidation product of $Fe^{(II)}EDTA$ and the dissolved oxygen.

The formation of SO_4^{2-} in the solution is not found in the absence of oxygen. This is demonstrated by the experiment shown in Fig. 7. The gas phase analysis in Fig. 7(a) exhibits a high degree of NO conversion and the formation of N_2O when the dithionite is consumed. As expected NO_2 cannot be detected. It should be pointed out that the formation of N_2 as a reaction product could not be confirmed in any of the experiments contrary to other statements in the literature [27, 28]. In this experiment the ratio of the absorbed NO to consumed $S_2O_4^{2-}$ is close to $[NO]/[S_2O_4^{2-}] \approx 1$. A quantitative analysis revealed that 42% of the NO is converted to NH_4^+ and 7% to $NH_2(SO_3H)$. Other possible reaction products, such as $HN(SO_3H)_2$, $N(SO_3H)_3$, $HN(SO_3H)OH$ and $N(SO_3H)_2OH$, could not be identified due to the lack of reference substances. The formation of these compounds by the absorption of NO on systems containing $Fe^{(II)}EDTA$ and sulfite in the solution has recently been demonstrated in the literature [29].

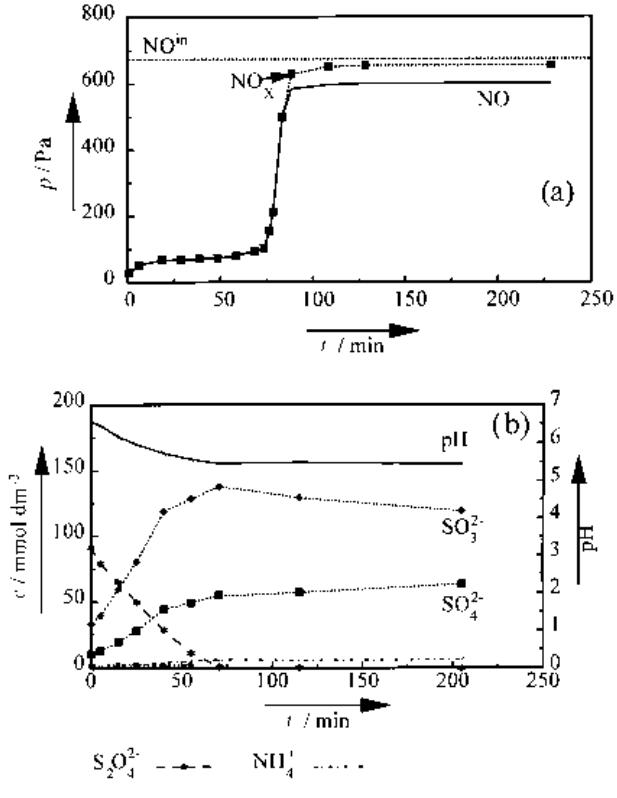

Fig. 6. Semibatch experiment of NO absorption with $Fe^{(II)}EDTA$ as the complexing agent and $S_2O_4^{2-}$ as the reducing agent: (a) gas-phase analysis and (b) solution analysis. System parameters: gas flow rate $q^g = 4.56\,dm^3\,min^{-1}$, volume of the liquid phase $V^l = 3.3\,dm^3$, gas holdup $\varepsilon = 0.046$, $T = 313\,K$, partial pressure of oxygen $p_{O_2} = 2.9\,kPa$, $c_{Fe^{(II)}EDTA} = 2.33\,mmol\,dm^3$, absorption liquid buffered with citric acid/citrate.

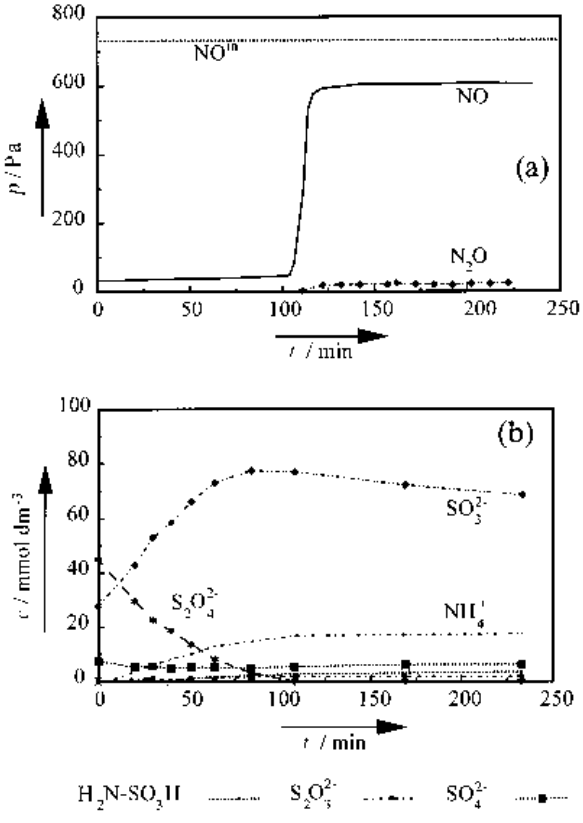

Fig. 7. Semibatch experiment of NO absorption with $Fe^{(II)}EDTA$ as the complexing agent and $S_2O_4^{2-}$ as the reducing agent: (a) gas-phase analysis and (b) solution analysis. System parameters: gas flow rate $q^g = 3.93\,dm^3\,min^{-1}$, volume of the liquid phase $V^l = 3.3\,dm^3$, gas holdup $\varepsilon = 0.045$, $T = 313\,K$, pH 6.4, $c_{Fe^{(II)}EDTA} = 2.62\,mmol\,dm^{-3}$, absorption liquid buffered with citric acid/citrate.

3.3. *Degree of NO conversion*

The degree of NO conversion X was found to be mainly dependent on the concentration of $Fe^{(II)}EDTA$ but not on that of dithionite. Figure 8 shows experimental results of NO conversion obtained with variable $Fe^{(II)}EDTA$ concentrations. At $[Fe^{(II)}EDTA] = 2 \times 10^{-3}\,mol\,dm^{-3}$ the degree of conversion attains a value of almost $X = 0.9$. Systematic investigations of the dependence of X on other system parameters, such as the partial pressure of NO, the gas flow rate q^g, and the temperature T

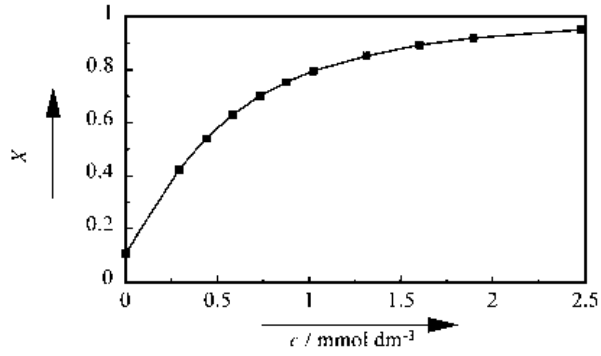

Fig. 8. Degree of NO conversion X with $S_2O_4^{2-}$ as function of the $Fe^{(II)}EDTA$ concentration. System parameters: gas flow rate $q^g = 3.93\,dm^3\,min^{-1}$, volume of the liquid phase $V^l = 3.3\,dm^3$, gas holdup $\varepsilon = 0.046$, $T = 313\,K$, pH 6.8, partial pressure of NO at the inlet $p_{NO} = 732\,Pa$.

have also been performed and the results are shown in Fig. 9(a)–(c). With increasing NO content and gas flow rate q^g the degree of conversion decreases due to kinetic limitation and decreasing residence time of NO in the gas/liquid contactor. The significant increase of X with the temperature T indicates that the complex kinetics of NO conversion with $Fe^{(II)}EDTA$ and dithionite is mainly reaction controlled.

A mathematical model which describes the steady state absorption process has been developed [20]. This model is based on the two-film theory and approximates the absorption column as a cascade of stirred tank reactors with first order reaction kinetics with respect to NO and $Fe^{(II)}EDTA$ and zero reaction order with respect to dithionite.

3.4. *Electrochemical regeneration of the redox mediator*

The kinetics of electrochemical dithionite regeneration by the cathodic reduction of sulfite was studied on lead electrodes in sulfate solutions at $4 \leq pH \leq 7$ and sulfite concentrations in the range of $2 \times 10^{-3} < c_{SO_3^{2-}} < 2 \times 10^{-2}\,mol\,dm^{-3}$ using the RDE. The overall reaction is

$$2HSO_3^- + 2H^+ + 2e^- \longrightarrow S_2O_4^{2-} + 2\,H_2O \qquad (7)$$

Figure 10 shows typical cathodic polarization curves at different rotation frequencies ω. At potentials $-1.2 < E_{SHE} < -0.45\,V$ the reduction process is mainly under limiting diffusion control (region II). In region I, the reaction proceeds under mixed diffusion and reaction control. The increase in the cathodic current density in region III is mainly due to the onset of the hydrogen evolution reaction. The base line curve in Fig. 10 obtained in the absence of SO_3^{2-} shows that the contribution of hydrogen evolution can be ignored in regions I and II.

Figure 11 shows the dependence of the limiting diffusion current density on the concentration of sulfite for two rotation frequencies at constant potential and pH. The linear dependence indicates that the electrochemical reaction corresponds to the sulfite reduction. Different reaction mechanisms are dis-

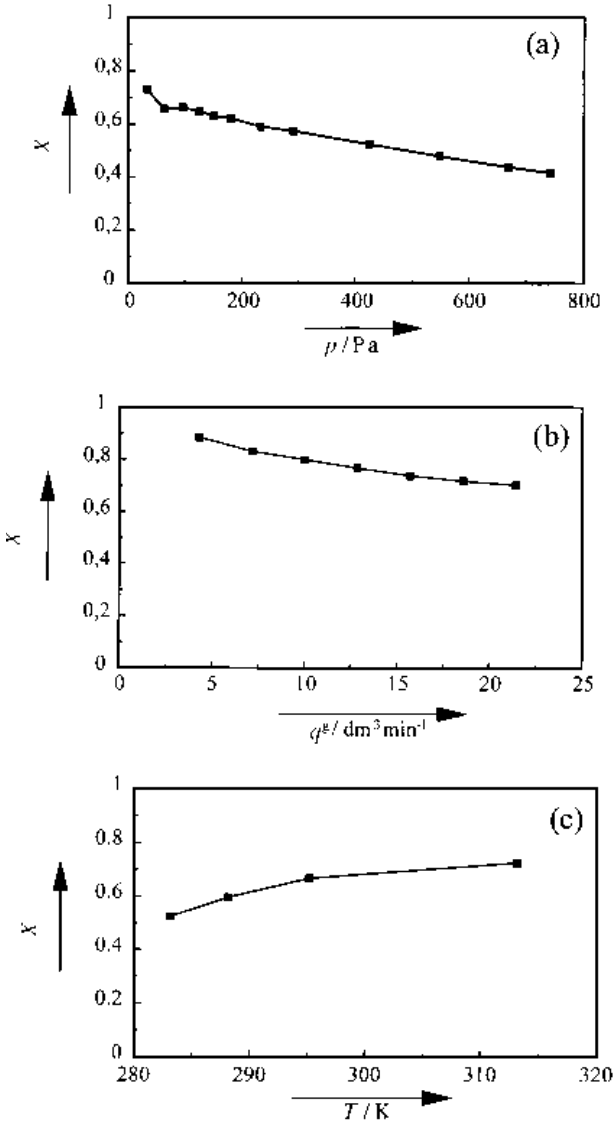

Fig. 9. Degree of NO conversion X as function of different system parameters: (a) partial pressure p of NO, (b) gas flow rate q^g, and (c) temperature T; constant parameters: volume of the liquid phase $V^l = 3.3\,dm^3$, pH ≈ 6.5. Other parameters: (a) $c_{Fe^{(II)}EDTA} = 0.29\,mmol\,dm^{-3}$, $q^g = 3.93\,dm^3\,min^{-1}$, $T = 313\,K$; (b) $c_{Fe^{(II)}EDTA} = 0.96\,mmol\,dm^{-3}$, $p_{NO}^{in} = 91\,Pa$, $T = 313\,K$; (c) $c_{Fe^{(II)}EDTA} = 0.96\,mmol\,dm^{-3}$, $p_{NO}^{in} = 732\,Pa$, $q^g = 3.93\,dm^3\,min^{-1}$.

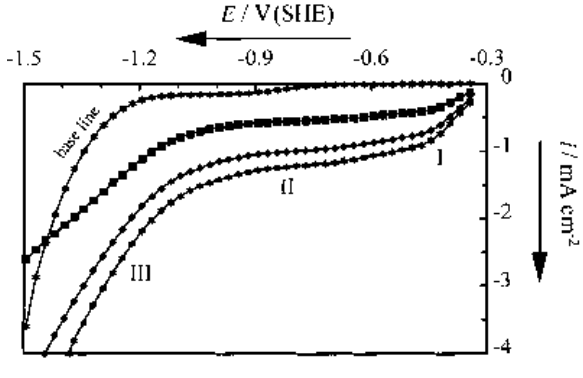

Fig. 10. Cathodic polarization curves of sulfite reduction on a lead electrode at different rotation frequencies, ω: (■) 9.42, (◆) 58.6 and (★) $107.8\,s^{-1}$. System parameters: electrolyte: 9.15×10^{-3} mol dm^{-3} HSO_3^-, 0. 2 mol dm^{-3} Na_2So_4, pH 4.55, T = 298K.

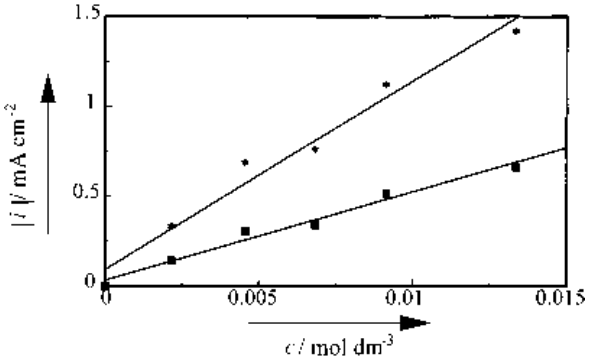

Fig. 11. Dependence of the limiting current density i on sulfite concentration. System parameters: $0.2\,\mathrm{mol\,dm^{-3}}$ Na_2SO_4, $E = -0.79\,\mathrm{V}$ vs SHE, pH 4.55, $T = 298\,\mathrm{K}$. Key : (■) $\omega = 9.42\,\mathrm{s^{-1}}$ and (★) $\omega = 107.3\,\mathrm{s^{-1}}$.

cussed in the literature [30], depending on the pH. In the pH range of $3.5 < \mathrm{pH} < 6$ the following mechanism was postulated by Kolthoff and Miller [31]

$$HSO_3^- + e^- \rightleftharpoons SO_2^- + OH^- \qquad (8)$$

$$2SO_2^- \rightleftharpoons S_2O_4^{2-} \qquad (9)$$

The cathodic current density can be expressed by the following formula:

$$i = \frac{-v_e F k^0 c_{HSO_3^-} \exp\left[-\frac{\alpha_c F}{RT}\left(E - E_0^0\right)\right]}{1 - 1.61\, D^{-2/3} \nu^{1/6} \omega^{-1/2} k^0 \exp\left[-\frac{\alpha_c F}{RT}\left(E - E_0^0\right)\right]} \qquad (10)$$

which is equivalent to the well known Frumkin equation [32] for a mixed charge transfer and diffusion controlled process. The first order reaction (8) is considered as the rate determining step and the reverse reaction is neglected.

Figure 12 shows experimental plots of i against $\sqrt{\omega}$ and optimum fit results using Equation 10. The shape of the experimental curves is well reproduced by the model simulation, however a quantitative agreement could not be achieved, which is also indicated by the fit parameters. The reason for this deviation may be the insufficient surface activity of the lead electrode or the possible dependence of the surface concentration of the reactant HSO_3^- on the surface pH which according to Equation 8 increases with the reaction rate, leading to a shift of the dissociation equilibrium

$$HSO_3^- + OH^- \rightleftharpoons SO_3^{2-} + H_20 \qquad (11)$$

to the right. At pH > 7.4 the reduction of hydrogen sulfite was found to disappear completely [33].

For technical applications the current efficiency Φ^e of the electrochemical generation of dithionite is of practical importance.

$$\Phi^e = \frac{c\,V\,v_e\,F}{I\,t} \qquad (12)$$

where V is the volume of the catholyte and I the current intensity. The concentration–time dependence of dithionite and sulfite obtained from experiments on a porous lead foam electrode in a divided cell using ion chromatography IC is shown in Fig. 13(a) and the corresponding current efficiency Φ^e is shown in Fig. 13(b). The decrease in SO_3^{2-} corresponds to the stoichiometric formation of dithionite $S_2O_4^{2-}$ according to Equation 7. The possible formation of thiosulfate $S_2O_3^{2-}$ was found to be negligible. The mean value of the current efficiency $\Phi^e = 0.8$ shows that lead works as a good electrode material for the formation of dithionite. The loss of 20% in current efficiency may be attributed to the formation of H_2. At extremely negative electrode potentials, $E_{SHE} = -1.8\,\mathrm{V}$, the formation of dithionite vanished completely, indicating the strong in-

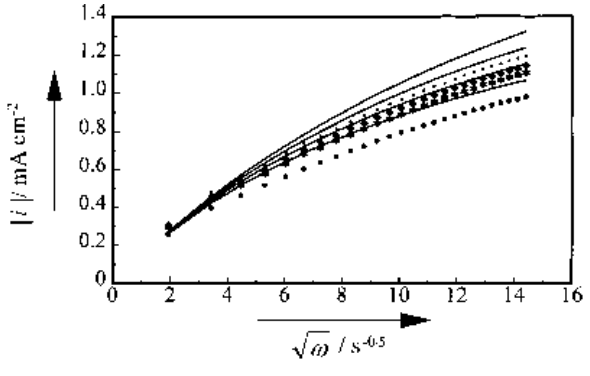

Fig. 12. Plots of experimental data i against $\sqrt{\omega}$ and optimum fits using Equation 10 for sulfite reduction at the rotating disc lead electrode. System parameters: $9.15 \times 10^{-3}\,\mathrm{mol\,dm^{-3}}$ HSO_3^-, $0.2\,\mathrm{mol\,dm^{-3}}$ Na_2SO_4, pH 4.55, $T = 298\,\mathrm{K}$. Parameters: diffusion coefficient D^{calc} : $1.52 \times 10^{-6}\,\mathrm{cm^2\,s^{-1}}$, mass transfer coefficient $k^0 = 4.38 \times 10^{-4}\,\mathrm{cm\,s^{-1}}$, symmetry factor $\alpha_c = 0.921$. E: (■) − 0.59, (◆) − 0.54, (★) − 0.49 and (●) − 0.44 V vs SHE.

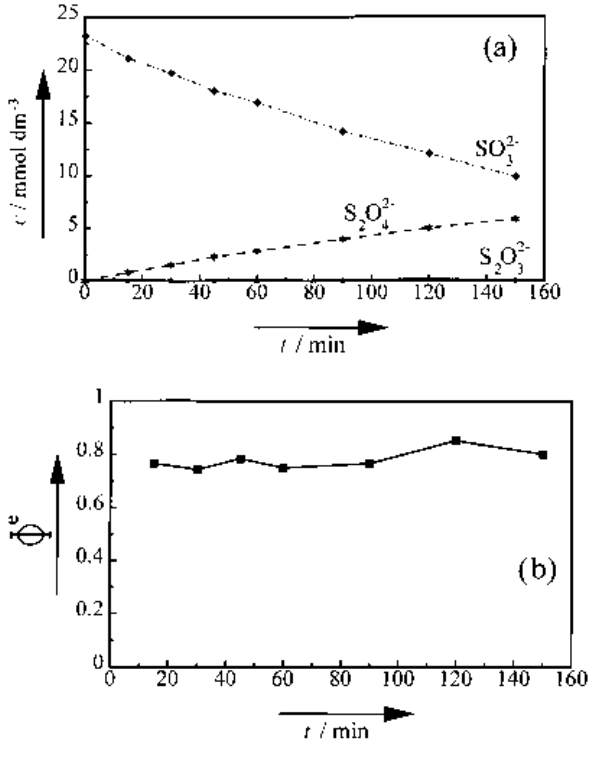

Fig. 13. Electrochemical regeneration of dithionite by reduction of sulfite using a porous lead foam electrode in a divided cell: (a) concentration-time dependence and (b) current efficiency as a function of polarization time. System parameters: $0.2\,\mathrm{mol\,dm^{-3}}$ Na_2SO_4, $E = -0.89\,\mathrm{V}$ vs SHE, pH 5.9, $T = 298\,\mathrm{K}$.

fluence of surface pH on this reaction. For technical applications, control of the solution pH and the electrode potential is therefore important.

3.5. *Combined NO-absorption and electrochemical dithionite regeneration*

To test the NO absorption under continuous operation, the absorption column was connected to a divided plate and frame cell (cf. Fig. 1). For the continuous regeneration of dithionite the absorption solution was pumped through the cathode compartment of the cell. Figure 14 shows the initial period of this experiment, when the electrochemical cell is not in operation and the absorption liquid contains only $Fe^{(III)}EDTA$ and sulfite. When the electrolysis current I is switched on at time t_1, the NO concentration drops sharply to a low value due to the formation of dithionite and remains at this level even after prolonged operation. The rate of NO conversion calculated from the partial pressure difference $\Delta p \approx 90\,\text{Pa}$ at $I \neq 0$ and the gas flow rate $q = 4.3\,\text{dm}^3\,\text{min}^{-1}$ is $2.7 \times 10^{-6}\,\text{mol}\,\text{s}^{-1}$. On the other hand, calculation of the Faradaic dithionite production from the applied current $I = 1.35\,\text{A}$ yields a value of $7 \times 10^{-6}\,\text{mol}\,\text{s}^{-1}$ with $v_e = 2$ for the overall reaction valency, cf. Equation 7. Assuming that each NO molecule consumes one $S_2O_4^{2-}$ in the conversion reaction (see the analysis of the experiment of Fig. 7) an overproduction of dithionite must be considered if a current efficiency of approx. $\Phi^e \approx 0.8$ is taken into consideration. This was also confirmed by solution analysis with regard to dithionite, indicating a satisfactory current yield for the indirect electrochemical process.

The performance of the NO absorption device was tested by varying the different system parameters. Figure 15 demonstrates the flexibility of the system. In this experiment oxygen was present at a certain level in the gas phase. Despite the 3 vol % O_2 the degree of NO conversion approaches almost 100% after switching on the electrolysis current at point 1 in

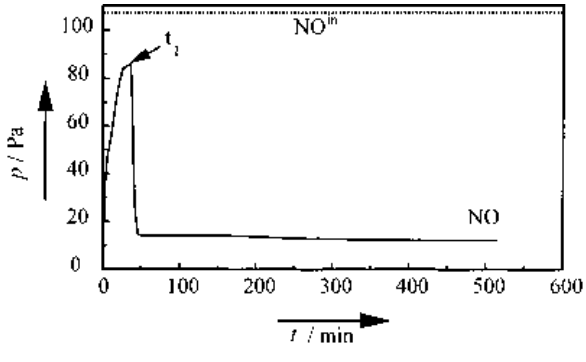

Fig. 14. NO absorption with electrochemical regeneration of the redox mediator dithionite in a divided plate and frame cell. System parameters: current intensity $I = 1.35\,\text{A}$ at $t \geq t_1$, $c_{Fe^{(III)}EDTA} = 1$ $\text{mmol}\,\text{dm}^{-3}$, gas flow rate $q^g = 4.3\,\text{dm}^3\,\text{min}^{-1}$, liquid flow rate $q^l = 55\,\text{dm}^3\,\text{h}^{-1}$, volume of the liquid phase $V^l = 3.7\,\text{dm}^3$, gas holdup $\varepsilon \approx 0.05$, $T = 313\,\text{K}$, initial sulfite concentration: $0.46\,\text{mol}\,\text{dm}^{-3}$.

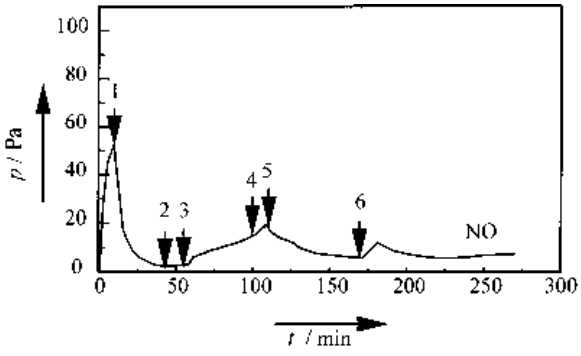

Fig. 15. NO absorption with electrochemical regeneration of the redox mediator dithionite in a divided plate and frame cell by varying the system parameters. Point (1) current intensity $I = 1.35\,\text{A}$, point (2) increase in O_2 partial pressure $p_{O_2} = 5.8\,\text{kPa}$, point (3) increase in NO partial pressure $p_{NO} = 200\,\text{Pa}$, point (4) increase in current intensity $I = 2.0\,\text{A}$, point (5) liquid flow rate $q^l = 100\,\text{dm}^3\,\text{h}^{-1}$, point (6) increase in the helium carrier gas stream $q^g = 7.1\,\text{dm}^3\,\text{min}^{-1}$. Initial system parameters: $I = 0\,\text{A}$, $c_{Fe^{(III)}EDTA} = 3\,\text{mmol}\,\text{dm}^{-3}$, gas flow rate $q^g = 4.3\,\text{dm}^3\,\text{min}^{-1}$, volume of the liquid phase $V^l = 3.7\,\text{dm}^3$, liquid flow rate $q^l = 55\,\text{dm}^3\,\text{h}^{-1}$, gas holdup $\varepsilon \approx 0.05$, $T = 313\,\text{K}$, pH 6.6, sulfite concentration: $0.36\,\text{mol}\,\text{dm}^{-3}$, dithionite concentration: $0\,\text{mol}\,\text{dm}^{-3}$, NO partial pressure $p_{NO} = 100\,\text{Pa}$, O_2 partial pressure $p_{O_2} = 3.1\,\text{kPa}$.

Fig. 15. Doubling the O_2 concentration (point 2) did not affect the degree of NO conversion. However, a significant increase in NO at the outlet was observed when the partial pressure of NO was doubled (point 3). An increase in current I by 50% (point 4) cannot counteract this effect. A more effective method is to increase the liquid flow rate q^l (point 5), leading to an enhancement of the mass transport controlled dithionite regeneration. Increasing the He carrier gas flow rate from $4.3\,\text{dm}^3\,\text{min}^{-1}$ to $7.1\,\text{dm}^3\,\text{min}^{-1}$ (point 6) has no effect on the steady state NO outlet concentration except for a short discontinuity in the system response.

On the basis of these experimental results and the theoretical model derived for the NO absorption [20], the following parameters, which are of technical importance, can be estimated. For a given normalized space velocity $v = q^g/V_R = 200\,\text{dm}^3\,\text{h}^{-1}\,\text{dm}^{-3}$ corresponding to $q^g = 15.7\,\text{dm}^3\,\text{min}^{-1}$, $V_R = 3.6\,\text{dm}^3$, and $Fe^{(II)}EDTA$ $14.8\,\text{mmol}\,\text{dm}^{-3}$ a degree of conversion $X = 0.92$ is calculated for a partial pressure of $p_{NO} = 120\,\text{Pa}$. Under these conditions a specific energy consumption of $E_S = 0.012\,\text{kWh}\,\text{m}^{-3}$ can be calculated for the electrolysis at a minimum current intensity $I = 2.3\,\text{A}$ at a typical value of the cell voltage $U_c = 5.2\,\text{V}$.

4. Conclusion

The present investigations demonstrate the feasibility of electrochemical processes for waste gas treatment. A high degree of NO conversion ($X > 0.9$) could be achieved by an indirect electrochemical reduction of NO with dithionite as the redox mediator and $Fe^{(III)}EDTA$ as the complexing agent in an outer cell process. The advantage of this technique is its high flexibility by which the process can be easily adapted

to various industrial conditions, in particular for small scale applications. Since the process temperature is below 100 °C it is also attractive for the treatment of waste gas emissions at low temperatures. Another inherent advantage is the fact that the redox mediator can be regenerated in an electrochemical step in contrast to conventional processes where large amounts of chemicals are consumed to keep the conversion process running. The process is easy to control by adjusting the cell voltage and electrolysis current, and is thus amenable to automation. Due to the low specific energy consumption the running costs are relatively low compared with other processes. Since the reaction products accumulating in the solution consist of reduced nitrogen compounds, a special solution treatment is necessary. Similar to the technique applied by the SNCR process the reduced nitrogen compounds can be converted to NH_2 radicals by injecting the solution into the hot zone of a burner ($T = 1200\,K$), leading to an additional NO reduction in the off gas according to the reaction

$$NH_2 + NO \longrightarrow N_2 + H_2O$$

This, however, needs further investigations.

Acknowledgement

The authors are indebted to the Commission of the European Community for financial support under contract No TPRO-CT92-0007.

References

[1] J. Kolar, 'Stickstoffoxide und Luftreinhaltung', Springer Verlag, Berlin (1990).
[2] J. Suhlmann and G. Motzoll, *Chem. Ing. Tech.* **64** (1992) 580.
[3] U. Cleve, Dokumentation Rauchgasreinigung in *BWK* **9** (1985) 24.
[4] B. von der Heide, *Energie* **6** (1990) 40.
[5] H. Menig, 'Emissionsminderung und Recycling', ecomed Verlag, Landsberg (1984).
[6] L. Himsel and P. Reichel, *VGB Kraftwerkstech.* **68** (1988) 56.
[7] H. J. Fischer, *Chem. Tech.* **10** (1981) 297.
[8] D. van Velzen, H. Langenkamp and A. Moryoussef, *J. Appl. Electrochem.* **10** (1990) 60.
[9] G. Kreysa, *Chem. Ing. Tech.* **62** (1990) 357.
[10] G. Kreysa and H.-J. Külps, *Ger. Chem. Eng.* **6** (1983) 325.
[11] G. Kreysa, *Dechema-Monographien* **109** (1987) 9.
[12] G. Kreysa, H.-J.Külps and C. Woebcken, *ibid.* **94** (1983) 199.
[13] S. E. Lyke and S. H. Langer, *J. Electrochem. Soc.* **138** (1991) 1682.
[14] G. Kreysa, M. Bisang, K. Kochanek and G. Linzbach, *J. Appl. Electrochem.* **15** (1985) 639.
[15] H. -J. Bart and K. Burtscher, *GÖCH-Schriftenreihe 'Umweltschutz'* **12** (1990) 215.
[16] G. Kreysa and A. Storck, *Dechema-Monographien* **123** (1991) 225.
[17] K. Jüttner, G. Kreysa, K.-H. Kleifges and R. Rottmann, *Chem. Ing. Tech.* **66** (1994) 82.
[18] M. Aurousseau, C. Roizard, A. Storck and F. Lapicque, *Ind. Eng. Chem. Res.* **35** (1996) 1243.
[19] R. Rottmann, 'Entwicklung und Untersuchung verschiedener Konzepte zur elektrochemischen SO_2-Entfernung aus Rauchgasen', Fortschr.-Ber. VDI Reihe 15 nr.111, VDI-Verlag, Düsseldorf (1993).
[20] K. -H. Kleifges, 'Entwicklung und Untersuchung verschiedener Konzepte zur elektrochemischen NO_x-Entfernung aus Rauchgasen', Fortschr.-Ber. VDI Reihe 15 nr.153, VDI-Verlag, Düsseldorf (1996).
[21] J. N. Armor, *J. Chem. and Eng. Data* **19** (1974) 82.
[22] R. H. Perry and D. W. Green, 'Perry's Chemical Engineers Handbook', McGraw-Hill, New York (1984) pp. 3–98.
[23] J. Seifert and G. Emig, *Chem. Ing. Tech.* **61** (1989) 560.
[24] W. Weisweiler, *Haus d. Tech. Vortr.-Veröff.* **500** (1986) 75.
[25] M. Schrod, J. Semel and R. Steiner, *Chem. Ing. Tech.* **57** (1985) 717.
[26] R. G. Rinker, T. P. Gorden, D. M. Mason, R. R. Sakaida and W. H. Corcoran, *J. Phys. Chem.* **64** (1960) 573.
[27] H. Jüntgen and E. Richter, Dokumentation Rauchgasreinigung in *BWK* **9** (1985) 8.
[28] D. W. DeBerry, *US Patent 4 126 529* (1978).
[29] H. Gutberlet, S. Finkler, B. Pätsch, R. van Eldik and F. Prinsloo, *VGB Kraftwerkstech.* **76** (1996) 139.
[30] S. I. Zhanov, 'Encyclopedia of the Electrochemistry of the Elements', Vol. IV-6 (edited by A. J. Bard), Marcel Dekker, New York (1975) p. 273.
[31] I. M. Kolthoff and C. S. Miller, *J. Amer. Chem. Soc.* **63** (1941) 2818.
[32] A. N. Frumkin and G. Tedoradse, *Z. Elektrochemie* **62** (1958) 251.
[33] W. L. Reynolds and Yu Yuan, *Polyhedron* **5** (1986) 1467.